Saturation and Multifractality of Lagrangian and Eulerian Scaling Exponents in Three-Dimensional Turbulence

Dhawal Buaria[1,2,*] and Katepalli R. Sreenivasan[1,3]

[1]*Tandon School of Engineering, New York University, New York, New York 11201, USA*
[2]*Max Planck Institute for Dynamics and Self-Organization, 37077 Göttingen, Germany*
[3]*Department of Physics and the Courant Institute of Mathematical Sciences, New York University, New York, New York 10012, USA*

(Received 10 July 2023; revised 11 September 2023; accepted 6 October 2023; published 14 November 2023)

Inertial-range scaling exponents for both Lagrangian and Eulerian structure functions are obtained from direct numerical simulations of isotropic turbulence in triply periodic domains at Taylor-scale Reynolds number up to 1300. We reaffirm that transverse Eulerian scaling exponents saturate at ≈2.1 for moment orders $p \geq 10$, significantly differing from the longitudinal exponents (which are predicted to saturate at ≈7.3 for $p \geq 30$ from a recent theory). The Lagrangian scaling exponents likewise saturate at ≈2 for $p \geq 8$. The saturation of Lagrangian exponents and transverse Eulerian exponents is related by the same multifractal spectrum by utilizing the well-known frozen hypothesis to relate spatial and temporal scales. Furthermore, this spectrum is different from the known spectra for Eulerian longitudinal exponents, suggesting that Lagrangian intermittency is characterized solely by transverse Eulerian intermittency. We discuss possible implications of this outlook when extending multifractal predictions to the dissipation range, especially for Lagrangian acceleration.

DOI: 10.1103/PhysRevLett.131.204001

Turbulent flows in nature and engineering comprise a hierarchy of eddies, with smaller eddies coexisting within larger ones and extracting energy from them. To understand the deformation and rotation of smaller eddies, the key mechanisms driving energy transfers, it is essential to examine the velocity increments across a smaller eddy of size $r \ll L$ (say), where L is the large-eddy size [1–3]. The longitudinal velocity increment $\delta u_r = u(x+r) - u(x)$ corresponds to the case when the velocity component $u(x)$ is in the direction of separation r. For velocity $v(x)$ taken orthogonal to r, transverse velocity increment $\delta v_r = v(x+r) - v(x)$ is obtained.

The motivation to study the small eddies (and hence velocity increments) stems from their purported universality, postulated by Kolmogorov (1941) [1]—K41 henceforth—which has since become the backbone of turbulence theory and modeling [3,4]. Building upon K41, one surmises that moments of increments $\langle (\delta u_r)^p \rangle$, called structure functions, follow a universal power-law scaling in the so-called inertial range

$$S_p(r) \equiv \langle (\delta u_r)^p \rangle \sim r^{\zeta_p}, \qquad \eta \ll r \ll L, \tag{1}$$

where η is the viscous cutoff scale. Establishing such a simple scaling enables dramatic simplification in studying a wide range of turbulent flows, and thus, structure functions have been of persistent interest and a cornerstone of turbulence theory [2,3,5,6]. K41 originally postulated $\zeta_p = p/3$; this result is known to be exact for $p = 3$, i.e., $\zeta_3 = 1$, but extensive studies from [7] to [8] (and others in between) have clearly established nonlinear deviations of ζ_p from $p/3$ for $p \neq 3$. This so-called anomalous scaling is attributed to the intermittency of interscale energy transfer processes (see, e.g., [2,3,5,6]).

Since turbulence can also be fundamentally explored from a Lagrangian viewpoint [2,9–12], forceful arguments can be similarly made for Lagrangian velocity increments $\delta u_\tau = u(t+\tau) - u(t)$ over time lag τ, measured along fluid-particle trajectories, and Lagrangian structure functions $\langle |\delta u_\tau|^p \rangle$ defined therefrom [13]. Extension of Kolmogorov phenomenology to Lagrangian increments gives

$$S_p^L(\tau) \equiv \langle |\delta u_\tau|^p \rangle \sim \tau^{\zeta_p^L}, \qquad \tau_\eta \ll \tau \ll T_L, \tag{2}$$

where the temporal inertial range is defined using T_L, the Lagrangian integral time, and τ_η, the timescale of viscous dissipation [2]. Since Lagrangian trajectories trace the underlying Eulerian field, it is natural to expect that a relation between Lagrangian and Eulerian exponents can be obtained.

Using K41, one obtains $\zeta_p^L = p/2$ [2]. However, experimental and numerical studies again show nonlinear deviations from this prediction [14–17]. Several attempts have been made [18–20] to quantify these deviations in terms of Eulerian intermittency, but they remain deficient for at least two reasons. First, the temporal scaling range in turbulence is substantially more restrictive than spatial scaling range [2,3], making it difficult to robustly extract the Lagrangian scaling exponents. Second, past attempts have overwhelmingly focused on characterizing Lagrangian intermittency from longitudinal Eulerian intermittency, assuming that longitudinal and transverse exponents are identical, despite counterevidence [21–26].

In this Letter, presenting new data from direct numerical simulations (DNSs) of isotropic turbulence at higher Reynolds numbers, we address both these challenges. We extract both Lagrangian and Eulerian scaling exponents. Our Eulerian results reaffirm recent results [8]. We then demonstrate an excellent correspondence between Lagrangian exponents and transverse Eulerian exponents, using as basis the same multifractal spectrum; this is different from the multifractal spectrum for longitudinal exponents, whose use in the past has failed to explain Lagrangian intermittency [14–17,27].

Direct numerical simulations.—The description of DNSs is necessarily brief here because they have been described in many recent works [28–33]. The simulations correspond to the canonical setup of forced stationary isotropic turbulence in a triply periodic domain and are carried out using the highly accurate Fourier pseudospectral methods in space and second-order Runge-Kutta integration in time; the large scales are numerically forced to achieve statistical stationarity [34,35]. A key feature of the present data is that we have achieved a wide range of Taylor-scale Reynolds number R_λ, going from 140 to 1300 (on grids of up to $12\,288^3$ points) while maintaining excellent small-scale resolution [29,36]. For Lagrangian statistics, a large population of fluid particles is tracked together with the Eulerian field. For $R_\lambda \leq 650$, up to 64M particles are tracked for each case, whereas for $R_\lambda = 1300$, 256M particles are tracked (with $\mathrm{M} = 1024^2$) [37–39], providing ample statistics for convergence.

Saturation of transverse exponents.—Anomalous scaling confers upon each moment order a separate and independent significance, instead of a mutual dependence (such as $\zeta_p = p/3$ based on K41). Multifractals have enjoyed considerable success in describing this behavior [3,6], but lack any direct connection to Navier-Stokes equations. Further, recent DNS at high R_λ have shown noticeable departures of ζ_p from multifractal predictions for high orders [8]. Instead, starting from Navier-Stokes equations, a recent theory [40] was able to provide an improved prediction for ζ_p. Additionally, this theory also predicts that longitudinal exponents saturate with the moment order, i.e., $\lim_{p\to\infty}\zeta_p \to$ constant.

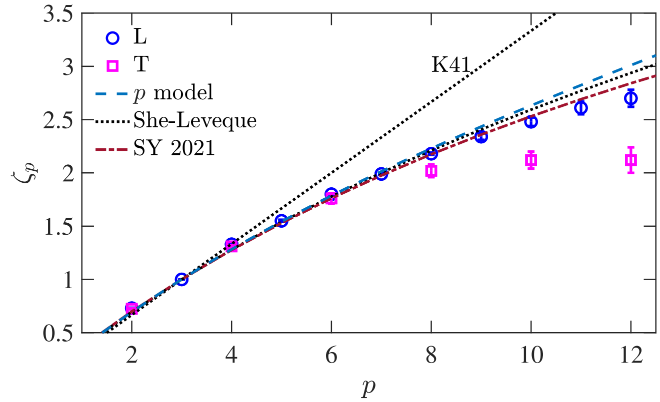

FIG. 1. Inertial-range scaling exponents for longitudinal and transverse Eulerian structure functions, the former from [8,40] and the latter from the present data (consistent with [8]). Various theoretical predictions [1,40,43,44] are also shown. The transverse exponents depart from all predictions and saturate.

Recall that the transverse exponents are defined by the relation $S_p^{\mathrm{tr}} \sim r^{\zeta_p^{\mathrm{tr}}}$, where $S_p^{\mathrm{tr}}(r) \equiv \langle |\delta v_r|^p \rangle$. (Absolute values are taken as the odd moments are zero from symmetry.) Multifractal models based on phenomenological considerations do not differentiate between longitudinal and transverse exponents, i.e., $\zeta_{2p}^{\mathrm{tr}} = \zeta_{2p}$, and general arguments have also been advanced to the same end [41,42]. However, several studies have persistently pointed out that the two sets of exponents are different [21–26]; recent work at high R_λ [8] has confirmed the differences, also showing that transverse exponents saturate: $\zeta_\infty^{\mathrm{tr}} \approx 2.1$ for $p \geq 10$. Incidentally, this saturation is very different from $\zeta_\infty \approx 7.3$ (for $p \geq 30$) predicted for longitudinal exponents in [40].

These findings are summarized in Fig. 1, showing the longitudinal and transverse exponents. Also included are K41 prediction, multifractal results [43,44], and the result from [40]. Important considerations go into establishing the reliability of high-order exponents with respect to statistical convergence, adequacy of grid resolution, and R_λ dependence. This discussion can be found in [8] and will not be repeated here. Instead, we focus on ζ_p^{tr}, which clearly depart from ζ_p and saturate for $p \geq 10$. The implication of different longitudinal and transverse exponents for small-scale universality is discussed later; we first demonstrate how ζ_p^{tr} is directly related to the Lagrangian exponents.

Lagrangian exponents from DNS.—Robust extraction of scaling exponents requires sufficient scale separation to allow a proper inertial range to exist. The Eulerian spatial scale separation for the highest $R_\lambda = 1300$ is $L/\eta \approx 2500$ [8], while the temporal range is $T_L/\tau_K \approx 105$ [45], thus making it inherently difficult to obtain a proper Lagrangian inertial range [46,47]. This difficulty is highlighted in Fig. 2, which shows the log local slope of $S_p^L(\tau)$

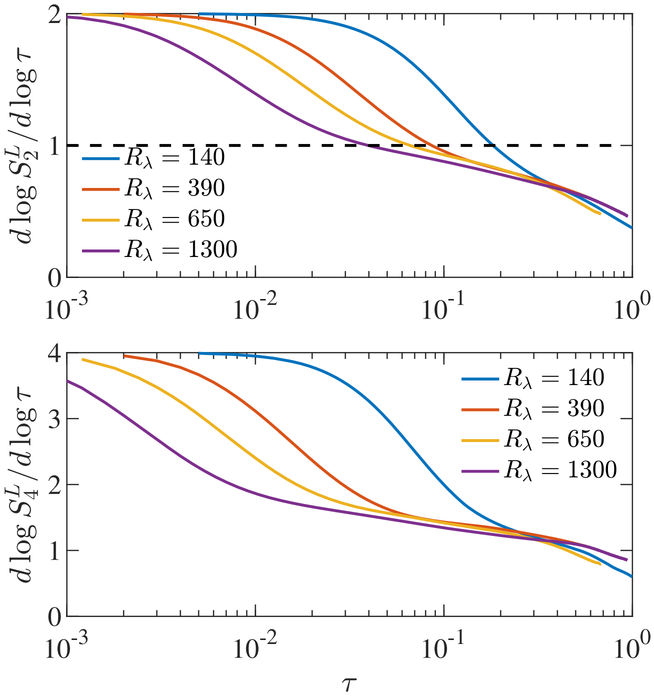

FIG. 2. Local slopes for second- (top panel) and fourth-order (bottom panel) Lagrangian structure functions at various R_λ.

at various R_λ, for $p = 2$ and 4 in top and bottom panels, respectively; although there is a suggestion of a plateau for the fourth order, the local slopes of the curves are still changing with R_λ. This is in contrast to the corresponding Eulerian result for $p = 2$, shown in Fig. 3, where a clear inertial range emerges with R_λ.

Because of this difficulty, Lagrangian exponents cannot be directly extracted even at the highest R_λ available. However, by using extended self-similarity [48], we can obtain the exponents with respect to the second order [17]. Figure 4 shows the ratio of local slope of $S_p^L(\tau)$ to that of $S_2^L(\tau)$. Evidently, a conspicuous plateau emerges for different orders in the same scaling range, seemingly independent of R_λ. Thus, we can extract the ratios ζ_p^L/ζ_2^L, which also was the practice in earlier works [15–17]. The justification for using ζ_2^L as the reference comes from the expectation $S_2^L \sim \langle\epsilon\rangle\tau$ [2]; since the mean dissipation appears linearly, the result $\zeta_2^L = 1$ is free of intermittency (akin to $\zeta_3 = 1$ for Eulerian exponents [49]).

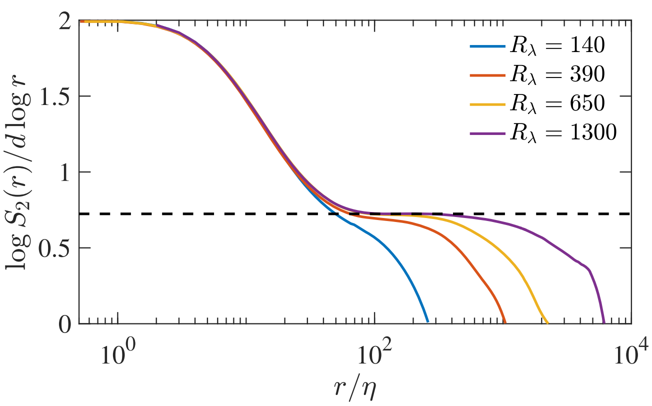

FIG. 3. Local slopes for the Eulerian second-order structure functions at different R_λ. In contrast to Lagrangian data in Fig. 2, a clear inertial range emerges with Reynolds number.

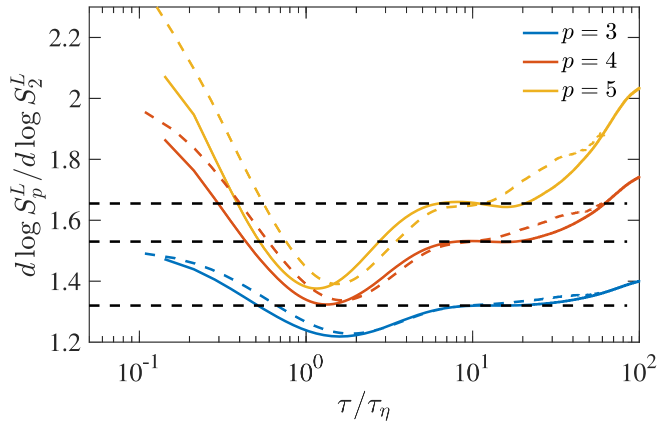

FIG. 4. Ratio of local slope for pth order Lagrangian structure function to second order, for $p = 3$–5, at $R_\lambda = 1300$ (solid lines) and $R_\lambda = 650$ (dashed lines).

Extending the procedure in Fig. 4, the ratios ζ_p^L/ζ_2^L are extracted for up to $p = 10$ and shown in Fig. 5. We also include earlier results from both experiments and DNS [15–17,20], obtained at comparatively lower R_λ. Overall, the current results at higher R_λ are in excellent agreement with prior results (which had larger error bars). A remarkable result, endemic to all cases, is that the Lagrangian exponents saturate for $p \gtrsim 8$, similar to the transverse Eulerian exponents in Fig. 1. The data in Fig. 5 are also compared with various predictions, which we discuss next.

The multifractal framework.—Evidently, the data in Fig. 5 strongly deviate from K41. Following [3,19], we

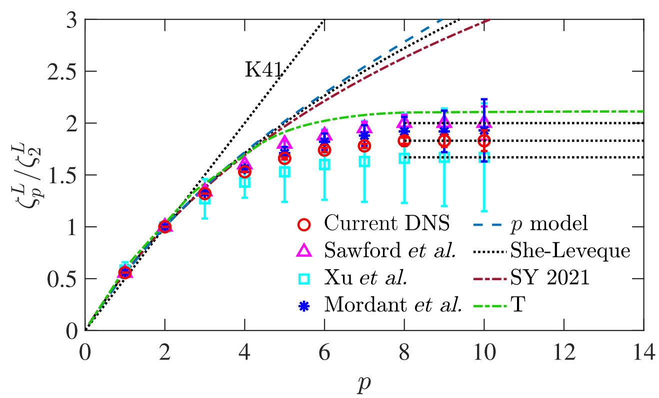

FIG. 5. Lagrangian scaling exponents and comparison with prior results and various multifractal models. The prediction from the transverse exponents is shown by the green curve (marked in legend by T) that saturates for large p.

will consider the well-known multifractal model for relating Eulerian and Lagrangian exponents. The key concept in multifractals is that the (Eulerian) velocity increment δu_r over a scale r is Hölder continuous, i.e., $\delta u_r \sim r^h$, where h is the local Hölder exponent with the multifractal spectrum $D(h)$ [3,50]. From this local scaling, Eulerian structure functions are readily derived by integrating over all possible h, as $\langle (\delta u_r)^p \rangle \sim \int_h r^{ph+3-D(h)} dh$. Using steepest-descent argument for $r \ll L$ gives

$$\zeta_p = \inf_h [ph + 3 - D(h)]. \quad (3)$$

The Lagrangian extension of multifractals relies on the phenomenological assumption that spatial and temporal separations are interchangeable: $r \sim \tau \delta u_r$, akin to frozen flow hypothesis, with $\delta u_r \sim \delta u_\tau$ [19]. This stipulation gives $\delta u_\tau \sim \tau^{h/(1-h)}$, resulting in the Lagrangian exponents

$$\zeta_p^L = \inf_h \left[\frac{ph + 3 - D(h)}{1-h} \right]. \quad (4)$$

Thus, Lagrangian exponents can be directly predicted using the Eulerian multifractal spectrum $D(h)$. Since past works have predominantly focused on Eulerian longitudinal exponents, with the implicit assumption that transverse exponents are same, the $D(h)$ of the longitudinal exponents has been used to infer Lagrangian exponents. However, such predictions do not work, as we see next.

The Lagrangian exponents can be computed from Eq. (4) by using Eulerian multifractal spectrum $D(h)$ from Eq. (3). The $D(h)$ corresponding to the Eulerian multifractal models shown in Fig. 1 are plotted in Fig. 6. They are obtained from ζ_p by taking a Legendre transform to invert the relations [3], giving

$$D(h) = \inf_p [ph + 3 - \zeta_p]. \quad (5)$$

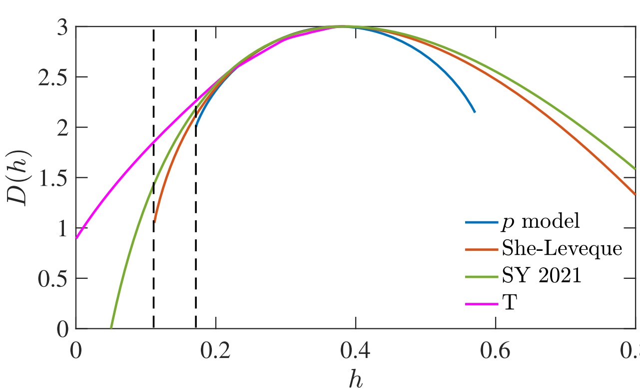

FIG. 6. The multifractal spectra for various models. The vertical dashed lines at $\frac{1}{3}\log_2(0.7)(\approx 0.17)$ and $\frac{1}{9}$ mark the minimum h allowed for p model [43] and She-Leveque [44], respectively, which preclude saturation; whereas $D(h=0) \approx 3 - 2.1 = 0.9$ marks saturation for transverse exponents at $\zeta_\infty^{\mathrm{tr}} \approx 2.1$.

For reference, the $D(h)$ for She-Leveque model is [44]

$$D(h) = 1 + c_1(h - h^*) - c_2(h - h^*) \log(h - h^*), \quad (6)$$

where $h^* = 1/9$, $c_1 = c_2(1 + \log\log\gamma - \log\gamma)$ and $c_2 = 3/\log\gamma$, with $\gamma = 3/2$. That for the Sreenivasan-Yakhot result of $\zeta_p = \zeta_\infty p/(p+\beta)$ [40] is

$$D(h) = 3 - \zeta_\infty - \beta h + 2\sqrt{\zeta_\infty \beta h}, \quad (7)$$

where $\zeta_\infty \approx 7.3$ and $\beta = 3\zeta_\infty - 3$. The result for p model can be found in [43].

In Fig. 6, in addition to the $D(h)$ from these known Eulerian cases, we also utilize Eq. (5) to numerically obtain the $D(h)$ for transverse exponents (with $\zeta_p^{\mathrm{tr}} \approx 2.1$ for $p \geq 10$, as shown in Fig. 1). Note, since the $D(h)$ for ζ_p^{tr} is obtained numerically, the inversion formula in Eq. (5) can only provide the concave hull [3]—which is what we plot in Fig. 6. The saturation value of exponents is reflected in the corresponding $D(h)$ curve for $h = 0$, as $D(0) = 3 - \zeta_\infty$ (≈ 0.9 for $\zeta_\infty^{\mathrm{tr}} \approx 2.1$). Note, $h < 0$ is not allowed in the multifractal framework [3]; the p model and She-Leveque results respectively correspond to $h_{\min} = \frac{1}{3}\log_2(0.7) \approx 0.172$ [43] and $h_{\min} = h^* = \frac{1}{9}$ [44], which preclude saturation. The Sreenivasan-Yakhot result [40] predicts saturation for longitudinal exponents at $\zeta_\infty \approx 7.3$, giving $D(0) = 3–7.3 = -4.3$ (not shown in Fig. 6).

Lagrangian exponents from the transverse multifractal spectrum.—As we saw, none of the multifractal predictions for Lagrangian exponents using Eulerian longitudinal exponents agree with the data. In contrast, the prediction corresponding to transverse Eulerian exponent (green dot-dashed line in Fig. 5) closely follows the measured results, particularly capturing the saturation at high orders. Note, the predicted saturation value $\zeta_\infty^L \approx 2.1$, is the same for both transverse Eulerian and Lagrangian exponents, The actual Lagrangian data saturate at a very slightly smaller value. We believe this minor difference (of only 5%) stems from the fact that even at $R_\lambda = 1300$, the temporal inertial range is underdeveloped, and the intermittency-free result of $\zeta_2^L = 1$ is not unambiguously realized. Since Lagrangian exponents shown in Fig. 5 are extracted as ratios ζ_p^L/ζ_2^L, this minor discrepancy in the saturation values could be explained by small departures from the expectation of $\zeta_2^L = 1$. Given this and also possible statistical uncertainties (at highest orders), the close correspondence between the transverse Eulerian exponents and Lagrangian exponents is quite remarkable.

It is worth noting that Lagrangian exponents saturate for slightly smaller p than for transverse Eulerian exponents. This readily follows from Eqs. (3) and (4) as a kinematic effect. For Eulerian exponents, $\zeta_3 = 1$ is exact, corresponding to $h \approx \frac{1}{3}$, $D(h) \approx 3$, which conforms to the intermittency-free K41 result [3]. This gives $\zeta_2^L = 1$ as the corresponding Lagrangian result for $h \approx \frac{1}{3}$, $D(h) \approx 3$. This argument can be extended to higher orders to show that Lagrangian exponents at order p correspond to transverse exponents at order $3p/2$. Thus, it follows that Lagrangian exponents saturate at smaller p. A similar correspondence can also be provided for other Lagrangian statistics, for instance, the second moment of acceleration (the temporal velocity gradient) corresponds to the third moment of spatial velocity gradients [2,27].

Discussion.—Two significant results emerge from our work: (a) scaling exponents saturate for both transverse Eulerian and Lagrangian structure functions, and (b) the saturation of Lagrangian exponents is characterized solely by the transverse Eulerian exponents (and not the longitudinal, as previously believed). Given that the transverse exponents are smaller for large p, this seems reasonable from the steepest-descent argument [3].

The saturation of scaling exponents is extreme form of anomalous behavior, but is not uncommon; it holds for Burgers equation [51] and passive scalar turbulence [52–54]. However, its prevalence in velocity field has become apparent only recently [8,40]. The theory of [40] predicts that Eulerian longitudinal exponents saturate as well, although at very high moment orders that cannot be yet validated. In contrast, both transverse Eulerian exponents and Lagrangian exponents saturate and at the same value of ≈2. Further, using a simple physical correspondence based on frozen flow hypothesis, they are related through the same multifractal spectrum (which differs from known spectrum for longitudinal Eulerian exponents). Interestingly, the saturation exponent of 2 implies a fractal codimension of 1 [3,6], suggesting that the saturation likely comes from localized (very) thin vortex filaments, which are known to be prevalent at the smallest scales [34,36,55].

Our results also bring forth some important questions. First is the extension of the multifractals from inertial to dissipative range, i.e., describing the scaling of velocity gradients. Such an extension relies on the phenomenological criterion that the local Reynolds number, describing the dissipative cutoff, is unity, i.e., $\delta u_r r/\nu = 1$ [3,40,56]. As highlighted in recent works [36,57], this is valid for longitudinal increments, but not for transverse increments, essentially because of how vorticity and strain rate interact in turbulence. It can thus be expected that the extension of multifractals to dissipation range works for longitudinal velocity gradients, but not for transverse velocity gradients. Since the current results suggest that Lagrangian intermittency is linked to transverse Eulerian intermittency, it follows that the extension to acceleration statistics would be an issue, as confirmed by our recent studies [27,58]. In addition, acceleration components are strongly correlated in turbulence [58,59], which is a feature of Navier-Stokes dynamics that is not accounted for by multifractals.

A second question concerns the meaning of universality given the longitudinal and transverse exponents behave differently. One strategy could be to consider a joint multifractal spectrum for longitudinal and transverse increments. It might be possible to set appropriate conditions on both to enable the inertial-range universality and the transition from the inertial to dissipation range. Essentially, addressing the discrepancy between longitudinal and transverse intermittency presents a critical and pressing problem in turbulence theory.

We gratefully acknowledge discussions with Victor Yakhot and sustained collaboration with P. K. Yeung. We also gratefully acknowledge the Gauss Centre for Supercomputing e.V. [60] for providing computing time on the supercomputers JUQUEEN and JUWELS at Jülich Supercomputing Centre (JSC), where the simulations reported in this Letter were primarily performed. Computations were also supported partially by the supercomputing resources under the Blue Water project at the National Center for Supercomputing Applications at the University of Illinois (Urbana-Champaign).

*Corresponding author: dhawal.buaria@nyu.edu

[1] A. N. Kolmogorov, The local structure of turbulence in an incompressible fluid for very large Reynolds numbers, Dokl. Akad. Nauk SSSR **30**, 299 (1941).

[2] A. S. Monin and A. M. Yaglom, *Statistical Fluid Mechanics* (MIT Press, Cambridge, MA, 1975), Vol. 2.

[3] U. Frisch, *Turbulence: The Legacy of Kolmogorov* (Cambridge University Press, Cambridge, England, 1995).

[4] S. B. Pope, *Turbulent Flows* (Cambridge University Press, Cambridge, England, 2000).

[5] A. N. Kolmogorov, A refinement of previous hypotheses concerning the local structure of turbulence in a viscous incompressible fluid at high Reynolds number, J. Fluid Mech. **13**, 82 (1962).

[6] K. R. Sreenivasan and R. A. Antonia, The phenomenology of small-scale turbulence, Annu. Rev. Fluid Mech. **29**, 435 (1997).

[7] C. W. Van Atta and J. Park, Statistical self-similarity and inertial subrange turbulence, in *Statistical Models and Turbulence: Proceedings of a Symposium held at the University of California, San Diego (La Jolla) July 15–21, 1971* (Springer, New York, 2005), pp. 402–426.

[8] K. P. Iyer, K. R. Sreenivasan, and P. K. Yeung, Scaling exponents saturate in three-dimensional isotropic turbulence, Phys. Rev. Fluids **5**, 054605 (2020).

[9] J. C. Wyngaard, Atmospheric turbulence, Annu. Rev. Fluid Mech. **24**, 205 (1992).

[10] B. L. Sawford, Turbulent relative dispersion, Annu. Rev. Fluid Mech. **33**, 289 (2001).

[11] G. Falkovich, K. Gawędzki, and M. Vergassola, Particles and fields in fluid turbulence, Rev. Mod. Phys. **73**, 913 (2001).

[12] F. Toschi and E. Bodenschatz, Lagrangian properties of particles in turbulence, Annu. Rev. Fluid Mech. **41**, 375 (2009).

[13] Absolute value is taken for Lagrangian increments since the odd moments are otherwise zero.
[14] B. L. Sawford, P. K. Yeung, M. S. Borgas, P. Vedula, A. L. Porta, A. M. Crawford, and E. Bodenschatz, Conditional and unconditional acceleration statistics in turbulence, Phys. Fluids **15**, 3478 (2003).
[15] N. Mordant, E. Lévêque, and J.-F. Pinton, Experimental and numerical study of the Lagrangian dynamics of high Reynolds turbulence, New J. Phys. **6**, 116 (2004).
[16] H. Xu, M. Bourgoin, N. T. Ouellette, and E. Bodenschatz (International Collaboration for Turbulence Research), High order Lagrangian velocity statistics in turbulence, Phys. Rev. Lett. **96**, 024503 (2006).
[17] B. L. Sawford and P. K. Yeung, Direct numerical simulation studies of Lagrangian intermittency in turbulence, Phys. Fluids **27**, 065109 (2015).
[18] M. S. Borgas, The multifractal Lagrangian nature of turbulence, Phil. Trans. R. Soc. A **342**, 379 (1993).
[19] L. Biferale, G. Boffetta, A. Celani, B. J. Devenish, A. Lanotte, and F. Toschi, Multifractal statistics of Lagrangian velocity and acceleration in turbulence, Phys. Rev. Lett. **93**, 064502 (2004).
[20] A. Arnéodo, R. Benzi, J. Berg, L. Biferale, E. Bodenschatz *et al.*, Universal intermittent properties of particle trajectories in highly turbulent flows, Phys. Rev. Lett. **100**, 254504 (2008).
[21] B. Dhruva, Y. Tsuji, and K. R. Sreenivasan, Transverse structure functions in high-Reynolds-number turbulence, Phys. Rev. E **56**, R4928 (1997).
[22] S. Chen, K. R. Sreenivasan, M. Nelkin, and N. Cao, Refined similarity hypothesis for transverse structure functions in fluid turbulence, Phys. Rev. Lett. **79**, 2253 (1997).
[23] S. Grossmann, D. Lohse, and A. Reeh, Different intermittency for longitudinal and transversal turbulent fluctuations, Phys. Fluids **9**, 3817 (1997).
[24] X. Shen and Z. Warhaft, Longitudinal and transverse structure functions in sheared and unsheared wind-tunnel turbulence, Phys. Fluids **14**, 370 (2002).
[25] T. Gotoh, D. Fukayama, and T. Nakano, Velocity field statistics in homogeneous steady turbulence obtained using a high-resolution direct numerical simulation, Phys. Fluids **14**, 1065 (2002).
[26] R. Grauer, H. Homann, and J.-F. Pinton, Longitudinal and transverse structure functions in high-Reynolds-number turbulence, New J. Phys. **14**, 063016 (2012).
[27] D. Buaria and K. R. Sreenivasan, Scaling of acceleration statistics in high Reynolds number turbulence, Phys. Rev. Lett. **128**, 234502 (2022).
[28] D. Buaria and K. R. Sreenivasan, Dissipation range of the energy spectrum in high Reynolds number turbulence, Phys. Rev. Fluids **5**, 092601(R) (2020).
[29] D. Buaria, E. Bodenschatz, and A. Pumir, Vortex stretching and enstrophy production in high Reynolds number turbulence, Phys. Rev. Fluids **5**, 104602 (2020).
[30] D. Buaria and A. Pumir, Nonlocal amplification of intense vorticity in turbulent flows, Phys. Rev. Res. **3**, L042020 (2021).
[31] D. Buaria, A. Pumir, and E. Bodenschatz, Generation of intense dissipation in high Reynolds number turbulence, Phil. Trans. R. Soc. A **380**, 20210088 (2022).
[32] D. Buaria and K. R. Sreenivasan, Intermittency of turbulent velocity and scalar fields using three-dimensional local averaging, Phys. Rev. Fluids **7**, L072601 (2022).
[33] D. Buaria and K. R. Sreenivasan, Forecasting small-scale dynamics of fluid turbulence using deep neural networks, Proc. Natl. Acad. Sci. U.S.A. **120**, e2305765120 (2023).
[34] T. Ishihara, T. Gotoh, and Y. Kaneda, Study of high-Reynolds number isotropic turbulence by direct numerical simulations, Annu. Rev. Fluid Mech. **41**, 165 (2009).
[35] R. S. Rogallo, Numerical experiments in homogeneous turbulence, NASA Technical Memo (1981), https://ntrs.nasa.gov/api/citations/19810022965/downloads/19810022965.pdf.
[36] D. Buaria, A. Pumir, E. Bodenschatz, and P. K. Yeung, Extreme velocity gradients in turbulent flows, New J. Phys. **21**, 043004 (2019).
[37] D. Buaria, B. L. Sawford, and P. K. Yeung, Characteristics of backward and forward two-particle relative dispersion in turbulence at different Reynolds numbers, Phys. Fluids **27**, 105101 (2015).
[38] D. Buaria, P. K. Yeung, and B. L. Sawford, A Lagrangian study of turbulent mixing: Forward and backward dispersion of molecular trajectories in isotropic turbulence, J. Fluid Mech. **799**, 352 (2016).
[39] D. Buaria and P. K. Yeung, A highly scalable particle tracking algorithm using partitioned global address space (PGAS) programming for extreme-scale turbulence simulations, Comput. Phys. Commun. **221**, 246 (2017).
[40] K. R. Sreenivasan and V. Yakhot, Dynamics of three-dimensional turbulence from Navier-Stokes equations, Phys. Rev. Fluids **6**, 104604 (2021).
[41] V. S. L'vov, E. Podivilov, and I. Procaccia, Invariants for correlations of velocity differences in turbulent fields, Phys. Rev. Lett. **79**, 2050 (1997).
[42] M. Nelkin, Multifractal scaling of velocity derivatives in turbulence, Phys. Rev. A **42**, 7226 (1990).
[43] C. Meneveau and K. R. Sreenivasan, Simple multifractal cascade model for fully developed turbulence, Phys. Rev. Lett. **59**, 1424 (1987).
[44] Z.-S. She and E. Leveque, Universal scaling laws in fully developed turbulence, Phys. Rev. Lett. **72**, 336 (1994).
[45] D. Buaria, Lagrangian investigations of turbulent dispersion and mixing using Petascale computing, Ph.D. thesis, Georgia Institute of Technology, 2016.
[46] B. L. Sawford and P. K. Yeung, Kolmogorov similarity scaling for one-particle Lagrangian statistics, Phys. Fluids **23** (2011).
[47] D. Buaria, Comment on "Universality and Intermittency of Pair Dispersion in Turbulence", Phys. Rev. Lett. **130**, 029401 (2023).
[48] R. Benzi, S. Ciliberto, R. Tripiccione, C. Baudet, F. Massaioli, and S. Succi, Extended self-similarity in turbulent flows, Phys. Rev. E **48**, R29 (1993).
[49] A. N. Kolmogorov, Dissipation of energy in locally isotropic turbulence, Dokl. Akad. Nauk SSSR **434**, 16 (1941).
[50] R. Benzi, G. Paladin, G. Parisi, and A. Vulpiani, On the multifractal nature of fully developed turbulence and chaotic systems, J. Phys. A **17**, 3521 (1984).
[51] J. Bec and K. Khanin, Burgers turbulence, Phys. Rev. **447**, 1 (2007).

[52] R. H. Kraichnan, Anomalous scaling of a randomly advected passive scalar, Phys. Rev. Lett. **72**, 1016 (1994).

[53] K. P. Iyer, J. Schumacher, K. R. Sreenivasan, and P. K. Yeung, Steep cliffs and saturated exponents in three-dimensional scalar turbulence, Phys. Rev. Lett. **121**, 264501 (2018).

[54] D. Buaria, M. P. Clay, K. R. Sreenivasan, and P. K. Yeung, Turbulence is an ineffective mixer when Schmidt numbers are large, Phys. Rev. Lett. **126**, 074501 (2021).

[55] J. Jiménez, A. A. Wray, P. G. Saffman, and R. S. Rogallo, The structure of intense vorticity in isotropic turbulence, J. Fluid Mech. **255**, 65 (1993).

[56] G. Paladin and A. Vulpiani, Degrees of freedom of turbulence, Phys. Rev. A **35**, 1971 (1987).

[57] D. Buaria and A. Pumir, Vorticity-strain rate dynamics and the smallest scales of turbulence, Phys. Rev. Lett. **128**, 094501 (2022).

[58] D. Buaria and K. R. Sreenivasan, Lagrangian acceleration and its Eulerian decompositions in fully developed turbulence, Phys. Rev. Fluids **8**, L032601 (2023).

[59] A. Tsinober, P. Vedula, and P. K. Yeung, Random Taylor hypothesis and the behavior of local and convective accelerations in isotropic turbulence, Phys. Fluids **13**, 1974 (2001).

[60] www.gauss-centre.eu.